Targeting TGFβ signaling pathway in fibrosis and cancer

Karkampouna, S.

Chapter 6

ALK1Fc suppresses tumor growth by impairing angiogenesis and affects cell proliferation of human prostate cancer cells *in vivo*

Eugenio Zoni[1,*], Sofia Karkampouna[2,*], Peter C. Gray[3], Marie Jose Goumans[2], Lukas J.A.C. Hawinkels[2], Gabri van der Pluijm[1], Peter ten Dijke[2] and Marianna Kruithof-de Julio[1,2,#].

[1]Dept. of Urology, Leiden University Medical Centre, Leiden, The Netherlands
[2]Dept. of Molecular Cell Biology, Leiden University Medical Centre, Leiden, The Netherlands
[3]Clayton Foundation Laboratories for Peptide Biology, The Salk Institute for Biological Studies, La Jolla CA, USA.
[*] Equally contributed, [#] Corresponding author

Manuscript submitted

Abstract

Prostate cancer is the second most common cancer in men worldwide and lethality is almost inevitable due to the consequences of metastasis. Therefore, targeting the molecular pathways that underlie primary tumor growth and spread of metastases is of great clinical value. Bone morphogenetic proteins (BMPs) play a critical role in prostate cancer. BMP9 and the closely related BMP10 signal via the transmembrane serine kinase receptors Activin receptor-Like Kinase 1 (ALK1) and ALK2 and the cytoplasmic proteins SMAD1 and SMAD5. The human ALK1 extracellular domain (ECD) binds BMP9 and BMP10 with high affinity and we show that a soluble chimeric protein consisting of the ALK1 ECD fused to human Fc (ALK1Fc) prevents activation of endogenous signaling via ALK1 and ALK2. We also show for the first time in prostate cancer that ALK1Fc reduces BMP9- mediated signaling and decreases tumor cell proliferation *in vitro*. In line with these observations, we demonstrate that ALK1Fc impairs angiogenesis and reduces tumor growth *in vivo*. Our data identify BMP9 as a putative therapeutic target and ALK1Fc as a potential therapy capable of targeting tumor cells and the supportive tumor angiogenesis. Together these findings justify the continued clinical development of drugs blocking ALK1 and ALK2 receptor activity.

Introduction

Prostate cancer is the second most common cancer in men worldwide[1]. The survival rate of prostate cancer patients is mostly determined by the extent of the tumor. If the cancer is restricted to the prostatic gland the median survival is estimated up to 5 years[2]. If prostate cancer has metastasized to distant organs, the current therapies are not curative and the median survival drops to 1 to 3 years[3]. Currently prostate cancer, when still in its first phase of androgen dependency, can be successfully treated surgically. Follow up with androgen deprivation therapy will then contain the cancer and reduce the possibility of metastasis[4,5]. However, once the cancer develops in an androgen-independent state, therapy is no longer useful or successful[5]. Risk of lethality rate is high due to the consequences of prostate cancer metastasis[6]. Indeed, the prognosis for patients diagnosed with metastatic disease has not markedly improved in recent decades, and metastases remain the direct cause of approximately 90% of cancer deaths[7]. Therefore, understanding the molecular pathways that underlie the emergence and spread of metastases from primary tumors are of great biological and clinical value.

Different lines of research have highlighted the role of the type I activin receptor–like kinase-1 (ALK1) of the transforming growth factor-β (TGFβ) pathway as key regulator of normal as well as tumor angiogenesis[8,9]. Bone morphogenetic protein-9 (BMP9) and BMP10 are high affinity ligands for ALK1, which is predominantly expressed by endothelial cells[10]. Alternatively, BMP9 signals through the BMP type I receptor ALK2[11-13]. Binding of BMP9/ BMP10 to ALK1/ ALK2 results in phosphorylation and activation of downstream effectors SMAD1 and/ or SMAD5[12-14]. BMP9 is produced in the liver, secreted in circulation[15] and it promotes liver cell proliferation of primary hepatocytes and human hepatoma HepG2 cells[16]. In ovarian cancer, BMP9 can act as proliferative factor, promoting human epithelial ovarian cancer and human immortalized ovarian surface epithelial cell proliferation through ALK2/ SMAD1/ SMAD4 pathway[13]. Similarly, BMP9 stimulates cell proliferation of liver cancer cells[17] and osteosarcoma growth[18]. Among the BMPs, BMP9 is the most recently identified[15] and least studied ligand. Current research has not only attributed a tumor promoter role to

BMP9[13,17,18] but also tumor suppressing properties[19-21] in different types of cancer, including prostate cancer.

Several studies have highlighted the role of BMP9/ ALK1 in the genetics and development of blood vessel formation, outlining its critical involvement in pathological and tumor angiogenesis[22,23]. Interestingly, alterations of signal transduction pathways that are important for blood vessel formation, such as the NOTCH pathway, have also been associated with arterio-venous malformations[24,25]. Recently, BMP9 and BMP10 signaling have been linked to NOTCH signaling, one of the major pathways involved in prostate cancer development, progression and bone metastasis[26]. Expression profiling studies have shown that members of NOTCH pathway are characteristic of high grade (Gleason 4+4=8) micro-dissected prostate cancer cells compared to low grade (Gleason 3+3=6)[27]. Moreover, inhibition of NOTCH1 reduces prostate cancer cell growth, migration and invasion[28]. Interestingly, NOTCH signaling pathway activates ALDH1A1, a well- known marker of prostate cancer stem cells[29-32].

In order to understand the role of BMP9 in prostate cancer tumor progression, we have employed here the soluble chimeric protein (ALK1Fc/ ACE-041)[33] containing the human ALK1 extracellular domain that binds with high affinity the ligands BMP9 and BMP10[34], thus, reducing activation of endogenous ALK1, ALK2 and downstream signaling[35]. BMP9 induces endothelial cell proliferation and vessel formation[36] while ALK1Fc has previously been shown to inhibit vascularization and tumor growth of breast cancer *in vivo* in an orthotopic transplantation model[34]. ALK1Fc binds and neutralizes only BMP9 and BMP10 ligands and not TGFβ3[4,35], which plays an important role in angiogenic processes. Phase I clinical trials have been completed using ALK1Fc as anti-angiogenesis therapy in myeloma (clinicaltrials.gov identifier NCT00996957).

Here we show, for the first time in prostate cancer, that ALK1Fc reduces BMP9 signaling and decreases cell proliferation of highly metastatic and tumor initiating human prostate cancer cells *in vitro*. We further demonstrate that ALK1Fc reduces tumor growth by impairing angiogenesis and affecting cell proliferation of human prostate cancer cells *in vivo*. Taken together these data suggest BMP9 as a possible therapeutic target and thus justifies the continued clinical development of drugs blocking ALK1 and ALK2.

Materials and Methods

Cell line and culture conditions

Human osteotropic prostate cancer cell lines PC-3M-Pro4luc2 cells[37] were maintained in Dulbecco's Modified Eagle Medium (DMEM) supplemented with 10% FetalClone II (FCII) serum (Thermo Fisher, Waltham MA, USA), 0.8 mg/ml Neomycin (Santacruz, Dallas, USA) and 1% Penicillin-Streptomycin (Life Technologies, Carlsbad, USA). C4-2B cells were maintained in T-medium DMEM (Sigma-Aldrich, the Netherlands) supplemented with 20% F-12K nutrient mixture Kaighn's modification (GibcoBRL, the Netherlands), 10% fetal calf serum (FCS) 0.125 mg/ml biotin, 1% Insulin-Transferin-Selenium, 6.825 ng/ml T3, 12.5 mg/ml adenine and 1% penicillin/streptomycin (all from (Life Technologies, Carlsbad, USA). Cells were maintained at 37°C with 5% CO_2.

Luciferase reporter gene constructs

PC-3M-Pro4Luc2 cells were seeded at a density of 50,000 cells in 500 µL medium in a 24-wells plate. Transient transfection of reporter constructs was performed with Lipofectamine2000 (Life Technologies, Carlsbad, USA) according manufacturer's protocol. For each well, 100 ng of NOTCH reporter RBP-Jk-luc,10 ng CAGGS-Renilla luciferase, 100 ng BRE renilla and 100 ng BRE-luc38 per well were transfected. After 24 hours, medium was replaced and cells were treated with BMP9 for 24 hours. The Firefly luciferase and Renilla luciferase levels in the lysates were measured using Dual Luciferase Assay (Promega, Madison, USA).

RNA isolation and Real-time qPCR

Total RNA was isolated with Trizol Reagent (Invitrogen, Waltham, USA) and cDNA was synthesized by treverse transcription (Promega, Madison, USA) according to manufacturer's protocol. qRT-PCR was performed with Biorad CFX96 system (Biorad, The Netherlands). Gene expression was normalized to *GAPDH* or *β-actin*. (For primer sequences see Supplementary Table I). Total RNA from frozen section (5µm) was isolated with Qiagen Mini Isolation kit (Qiagen, the Netherlands) according to manufacturer protocol. Primer sequences are listed in Table 1.

MTS assay

Cells were seeded at density of 2.000 cells/ well, in 96- well plates and treated with ALK1Fc or control-Fc (CFc) (10ug/ml, Acceleron, USA) allowed growing for 24, 48, 72 and 96 hours. After incubation, 20 µl of 3-(4,5 dimethylthiazol- 2- yl)- 5 -(3 -carboxymethoxyphenyl)- 2 -(4 -sulfophenyl)- 2 H-tetrazolium was added and metabolic activity (absorbance of formazan product at 490nm) was measured after 2 hours incubation at 37°C. MTS absorbance values are positively proportional to total number of metabolically active cells providing an indirect correlation with cell proliferation rate[39] (CellTiter96 Aqueous Non-radioactive Cell proliferation assay, Promega).

Animals

Male, 6-8 week-old, athymic nude mice (Balb/c nu/nu), purchased from Charles River (L'Arbresle, France), were used in all *in vivo* experiments (n=15 per group). Mice were housed in individual ventilated cages under sterile condition, and sterile food and water were provided ad libitum. Animal experiments were approved by the local committee for animal health ethics and research of Leiden University (DEC #11246), and carried out in accordance with European Communities Council Directive 86/609/EEC. After the experimental periods, mice were injected with hypoxia probe (6mg/kg, Burlington, Massachusetts, USA) and lectin-Tomato (1mg/kg, Vector Laboratories, USA) intravenously prior to perfusion and sacrified according to our mouse protocol. Tumors were dissected and processed for further histomorphological analysis as described below.

Orthotopic prostate transplantation and ALK1Fc treatment

A total of 25.000 PC-3M-Pro4luc2 cells (10ul final volume) were injected in the dorsal lobe

of nude mice. In brief: after anesthetizing the mice with isoflurane, each mouse was placed on its back and a small incision was made along the lower midline of the peritoneum for about 1 cm. The prostate dorsal lobes were exteriorized and stabilized gently. A 30-gauge needle attached to a 1-cc syringe was inserted into the right dorsal lobe of the prostate and 10 µl of the material were slowly injected. A well-localized bleb indicates a successful injection. After retracting the needle a Q-tip was placed over the injection site for about 1 min to prevent bleeding and spillage of material. The prostate was then returned to the peritoneum and the abdominal wall and skin layer was sutured. After establishment of the primary tumor, at 10 days after the orthotopic transplantation, mice were intraperitoneally injected with Control-Fc (CFc) or ALK1Fc compounds (1mg/kg) twice per week.
Administration of compounds was performed for four weeks. ALK1-Fc is a fusion protein comprised of the extracellular domain of human ALK1 fused to the Fc region of IgG and was obtained from Acceleron Pharma, Cambridge, USA. The Fc domain of IgG1 was used as a control (MOPC-21; Bio Express, West Lebanon NH).

Whole body bioluminescent imaging (BLI)

Tumor growth was monitored weekly by whole body bioluminescent imaging (BLI) using an intensified-charge-coupled device (I-CCD) video camera of the *in vivo* Imaging System (IVIS100, Xenogen/Perkin Elmer, Alameda, CA, USA) as described previously[40]. Mice were anesthetized using isoflurane and injected intraperitoneally with 2mg D-luciferin (Perbio Science, the Netherlands). Analyses for each metastatic site were performed after definition of the region of interest and quantified with Living Image 4.2 (Caliper Life Sciences, Belgium). Values are expressed as relative light units (RLU) in photons/sec.

Immunofluorescence

Immunofluorescence staining was performed as described previously[41]. In brief, 5-µm paraffin embedded sections were used. For antigen retrieval, sections were boiled in antigen unmasking solution (Vector Labs, Peterborough, UK) and stained with following antibodies, CD31 (Sigma), ALDH1A1 (Abcam), phosphoHistone 3 (Millipore) and cleaved Caspase 3 (Cell Signaling). Sections were blocked with 1% bovine serum albumin (BSA)- PBS-0.1% v/v Tween-20 and incubated with primary antibodies diluted in the blocking solution, overnight at 4°C or room temperature. Sections then were incubated with secondary antibodies labelled with Alexa Fluor 488, 555, or 647 (Invitrogen/Molecular Probes, Waltham, MA, USA) at 1:250 in PBS-0.1% Tween-20. Nuclei were visualized by TO-PRO-3 (Invitrogen/Molecular Probes, 1:1000 diluted in PBS-0.1% Tween-20) or DAPI which was included in the mounting medium (Prolong G, Invitrogen/Molecular Probes).

Western immunoblotting

Proteins were extracted by using RIPA buffer (Thermo Scientific) and protein concentrations were quantified according to manufacturer's protocol (Thermo Scientific). Proteins samples (20 µg per sample) were separated by 15% SDS- PAGE followed by transfer to a blotting membrane. The membrane was blocked with 5% Milk, dissolved in PBS-Tween-20 for 1 hour at room temperature. The membrane was incubated with 1:1000 primary antibody (anti-NOTCH1, Cell Signaling, catalogue number 3608) at 4°C overnight. Subsequently, the

membrane was incubated with 1:10000 secondary horseradish peroxidase (HRP) antibody. All antibodies were dissolved in PBS-Tween-20. Chemi-luminescence was used to visualize the bands.

Statistical analysis

Statistical analysis was performed with GraphPad Prism 6.0 (GraphPad software) using t-test or ANOVA for comparison between more groups. Data is presented as mean ± SEM. P-values ≤ 0.05 were considered to be statistically significant (* $P < 0.05$, ** $P < 0.01$, *** $P < 0.001$).

Results

ALK1Fc reduces primary prostate tumor burden *in vivo*

To investigate the role of BMP9 in prostate cancer progression, the BMP9- ligand trap, ALK1Fc, was administered in a mouse model of orthotopic prostate cancer. Orthotopic prostate tumor growth was induced by intra-prostatic inoculation of human prostate cancer PC-3M-Pro4luc2 cells in Balb/c nude mice and tumor progression was followed by bioluminescence imaging (BLI)37 (**Fig.1A**). Based on the BLI signal the mice were distributed between two treatment groups; ALK1Fc or CFc (n=15 per group). The compounds were injected twice weekly and tumor imaging and body weights were monitored weekly for 5 weeks (**Fig.S1**). Tumor burden was quantitatively assessed for each animal during the course of treatment. The group of animals that received ALK1Fc exhibit smaller tumor size compared to the animals that received CFc based on the size after resection (**Fig.1B**) and bioluminescence quantification (**Fig.1C**, $p<0.05$).

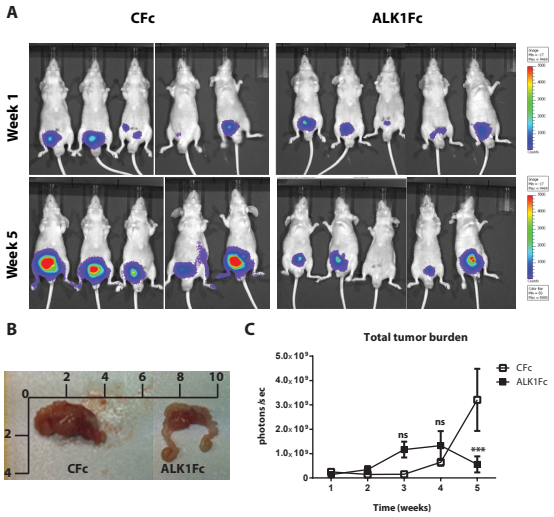

Fig.1. Effect of ALK1Fc *in vivo*
(A). PC-3M-Pro4Luc2 cells were orthotopically injected in the anterior lobe of prostate gland of nude mice (n=15 per group). Detection of primary tumor burden was observed at 2 weeks after injection, time point designated as "week 1" at the start of treatment with ALK1Fc or CFc. Representative examples of bioluminescent images of tumor burden at the start of treatment with ALK1Fc/ CFc (week 1) and at the end point (week 5). (B). Representative images of primary tumor size from a recipient of CFc versus ALK1Fc treatment after 5 weeks. (C). Quantification of bioluminescent signal (photons/sec) in mice treated with either CFc (n=14) or ALK1Fc (n=15) for 5 weeks. P value <0.001 (***).

Effect of ALK1Fc in vascular density, hypoxia and cell proliferation of the primary prostate tumor

The acquisition of tumor angiogenesis promotes tumor growth beyond a few mm^3 sizes. Intravital lectin perfusion was used to map the perfused elements of the tumor vasculature in mice. Fluorescent-conjugated lectin (lectin-Tomato) was visualized in tumor tissue sections and quantified. Vascular density, indicated by the overall lectin presence, was overall decreased in the tumors treated with ALK1Fc compared to the CFc group (**Fig. 2A-B**; p value= 0.058 statistically not significant). We evaluated the presence of endothelial cells in tumor sections by CD31 immunofluorescence. CD31 expression in tumors showed decreased trend after treatment with ALK1Fc which could indicate fewer endothelial cells and vessels (**Fig. 2C-D**; p value= 0.052, statistically not significant). Hypoxia is an important component of angiogenesis and critical for tumor formation. A hypoxia-induced fluorescent probe was injected in tumor bearing mice prior to sacrifice and the hypoxic areas within the tumors were visualized after tumor resection (**Fig.2E-F**). Hypoxic areas are found in both treatment groups; however, the overall amount of hypoxia seems higher in ALK1Fc-treated, tumor-bearing mice over the CFc-treated groups (**Fig.2E-F**; p=0.05, non-significant). We assessed the presence of total cell proliferation and cell death in these tumors by immunofluorescence for mitosis marker, phosphorylated histone 3 (PH3), and apoptosis marker, cleaved caspase 3 (CASP3). Dividing PH3 positive cells are predominantly located in normoxic areas (**Fig.2E**, left panel). Quantification of immunofluorescence signal shows that the number of dividing cells is significantly lower in the ALK1Fc-treated animals (**Fig.2G**; $p<0.05$). Total amount of apoptotic cells (Caspase-3 positive) is significantly higher in the ALK1Fc-treated tumors (**Fig.2H**; $p<0.05$). Histological analysis indicates localization of apoptotic cells mostly, however not exclusively, in the hypoxic areas (**Fig.2E**), suggesting a correlation between hypoxia and tumor cell death.

ALK1Fc decreases proliferation of human prostate cancer cells

To investigate the effect of ALK1Fc on prostate cancer cells we first measured the mRNA levels of BMP9 type I receptors ALK1 and ALK2 in PC-3M-Pro4Luc[237] human prostate cancer cell line and tested their response to BMP9. As previously reported in highly metastatic PC-3 and PC-3M prostate cancer cells[42], qRT-PCR analysis in osteotropic PC-3M-Pro4Luc2 cells revealed undetectable levels of ALK1 mRNA and mRNA expression of ALK2 (**Fig.S2A**). Treatment with BMP9 showed a dose-dependent induction of BRE-Renilla luciferase activity ($p<0.01$ and $p<0.05$ with 0.5nM and 1 nM BMP9, respectively) indicative of conserved and active signaling machinery (**Fig.S2B**). Using the 1nM BMP9 dose for subsequent experiments, we tested the individual effect of CFc and ALK1Fc or the combined effect of BMP9 with either ALK1Fc or CFc on BRE reporter assay (**Fig.S2C**). Treatment with ALK1Fc (10ug/ml) completely abolished the BMP9-mediated BRE luciferase (luc) activity (**Fig.S2C**; BMP9+ALK1Fc) to levels similar to the non-stimulated control (Untreated). Treatment with BMP9+CFc (10ug/ml) led to induction of BRE-luc activity of similar level as the BMP9 treatment (**Fig.S2C**; p-value <0.05). Taken together, these results indicate that ALK1Fc blocks ALK2-mediated BMP9 signaling in PC-3M-Pro4Luc2 cells. The functional effect of ALK1Fc on human prostate cancer cells was investigated by measuring metabolic activity by accumulation of MTS substrate, indicative of cell growth rate (proliferation). BMP9 stimulation *in vitro* led to increase of MTS absorbance indicating higher cell number (**Fig.3A**). Treatment with 10ug/ml ALK1Fc, but not

with control Fc (CFc), reduced BMP9-induced PC-3M-Pro4Luc2 cell proliferation ($p<0.001$ at day 4 comparing vehicle versus BMP9 or ALK1Fc treatment, respectively) (**Fig.3A**). Effect of only ALK1Fc or CFc on MTS assay was also assessed in absence of exogenously-added BMP9 and showed no influence of these compounds on the basal cell growth levels (**Fig. S2D**). The BMP9 effect of was also tested in the C4-2B prostate cancer cell line; however no significant difference in MTS assay was measured (**Fig.S2E**). Additionally, BMP9 treatment in PC-3M-Pro4Luc2 cells combined with ALK2 functional inhibition by small molecule BMP type I receptor inhibitor LDN193189 (LDN) [43,44] showed abolishment of BMP9-induced proliferation (**Fig.3B**). LDN effectively blocked the activity of the BRE-luc reporter after BMP9 stimulation of PC-3M-Pro4 cells (**Fig.S2F**) and the effect of LDN showed minimal impact on basal cell proliferation levels in absence of exogenously added BMP9 (**Fig.S2G**). Finally, we evaluated the clonogenic ability of PC-3M-Pro4Luc2 cells after BMP9 treatment alone (**Fig.S3A**) and confirmed that BMP9 affects cell growth, strongly increasing the size of the colonies (**Fig.S3B**, $p<0.05$). However, BMP9 showed no effect on colony formation/ self-renewal ability of PC-3M-Pro4Luc2 since the total number of colonies formed is similar (**Fig.S3C**). Together, these data indicate that ALK1Fc strongly reduces BMP9-induced cell proliferation of human prostate cancer cells.

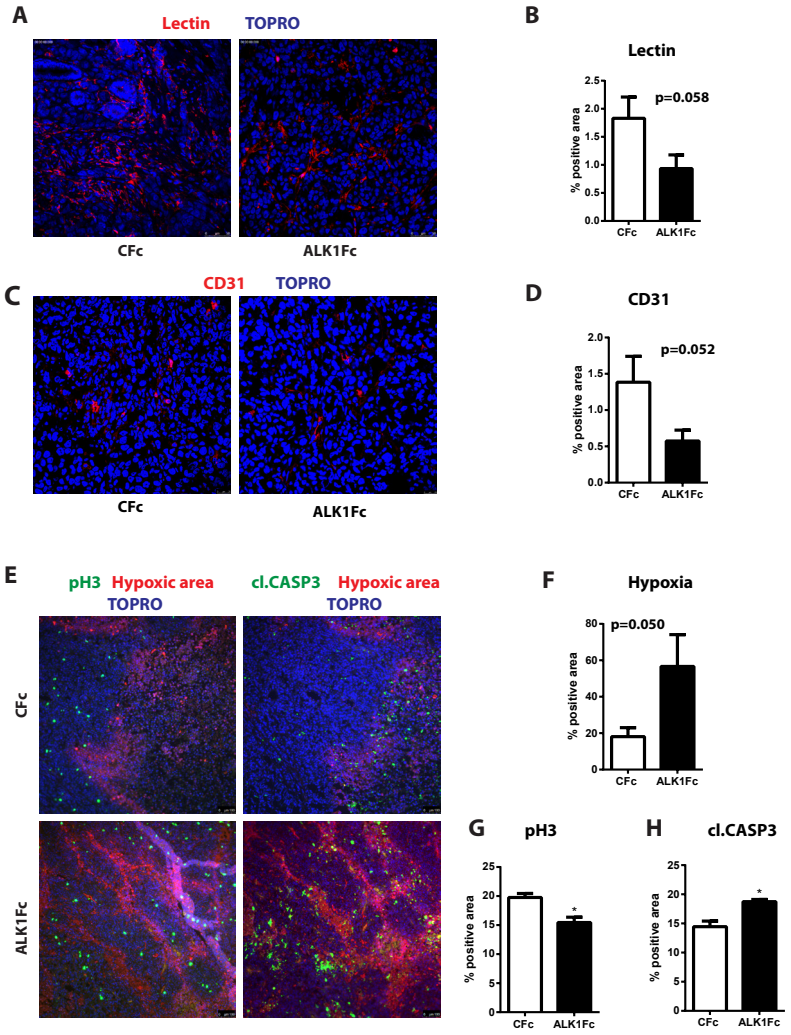

Fig.2. Effect of ALK1Fc on vascular density, cell proliferation and apoptosis *in vivo*

(A). Representative images of lectin detection in primary prostate tumor samples after perfusion with lectin-DsRed (red). TOPRO (blue) marks the nuclei. Treatment groups: ALK1Fc or CFc. (B). Quantification of lectin positive surface area in all tumor samples of each group (n=14 CFc group, n=15 ALK1Fc group) (C). Representative images of CD31 (green) immunofluorescence staining in primary prostate tumor samples after 5 weeks of treatment with either ALK1Fc or CFc. (D). Quantification of CD31 positive surface area in all tumor samples of each group (n=14 CFc group, n=15 ALK1Fc group). (E). Representative images of hypoxia immunofluorescence staining (red) in primary prostate tumor samples after 5 weeks of treatment with either ALK1Fc or CFc. Hypoxia probe was injected prior to sacrifice and was detected by a specific fluorescent antibody. White lines are used to arbitrarily distinguish the hypoxic (red) area from the non-hypoxic one. Immunofluorescence images for colocalization of apoptotic or proliferating cells in hypoxic/ normoxic area within the prostate tumor area in ALK1Fc and CFc treated animals. pH3: Phosphorylated Histone 3 cell proliferation marker (green); cleaved caspase 3 apoptosis marker (green); Hypoxic probe-antibody; hypoxic area (red). (F). Quantification of hypoxia positive area in all tumor samples of each group (n=15 per group). (G). Quantification of total pH3 positive area in all tumor samples of each group (n=14 CFc group, n=15 ALK1Fc group). (H). Quantification of total cleaved caspase 3 positive (apoptotic cells) in all tumor samples of each group (n=14 CFc group, n=15 ALK1Fc group).

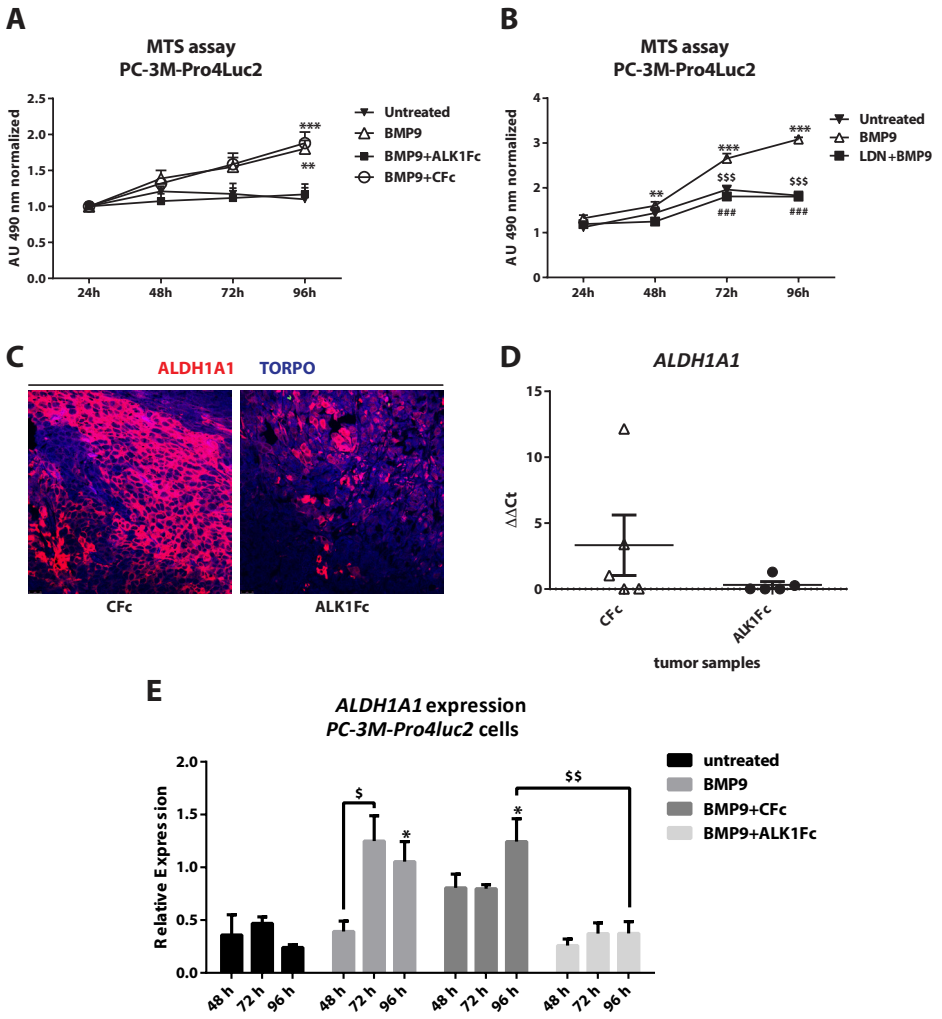

Fig.3. Effect of BMP9 and ALK1Fc on proliferation and ALDH1A1 expression

(A). Cell proliferation MTS assay (24, 48, 72, 96 hours) was performed in PC-3M-Pro4Luc2 cells stimulated with recombinant BMP9 (1nM), BMP9 (1nM)+ALK1Fc (10ug/ml) or BMP9 (1nM)+CFc (10ug/ml). Accumulation of MTS was measured based on absorbance at 490 nm. Values are normalized to the basal measurements at 24 hours after cell seeding and treatments. Graph represents values for three independent experiments (n=3). Error bars indicate ± SEM. P value < 0.01 (**) BMP9 versus Untreated and P-value < 0.001 (***) BMP9+CFc versus Untreated. (B). Cell proliferation assessed by MTS assay (24, 48, 72, 96 hours). PC-3M-Pro4Luc2 cells were seeded at low density in 96-well plates and treated with BMP9 (1nM) and in combination with LDN (BMP type I receptor inhibitor LDN193189, 120nM) (LDN+BMP9). (n=2). Error bars indicate SEM. (C). Representative images of ALDH1A1 immunofluorescence in prostate tumor samples from ALK1Fc and CFc treated animals. ALDH1A1: red; TOPRO: blue nuclear dye. (D). Quantification of ALDH1A1 mRNA by Q-PCR in tumor samples of each group (n=5 for CFc, n=5 for ALK1Fc). (E). Expression of ALDH1A1 in PC-3M-Pro4Luc2 cells. Relative mRNA expression was measured by Q-PCR from cDNA obtained from PC-3M-Pro4Luc2 cells treated with BMP9, BMP9+ALK1Fc, BMP9+CFc, for 48, 72 and 96 hours. Values are normalized to β-actin expression. Error bars are ±SEM (n=3).

Expression of BMP9, ALK1 and ALK2 in human and murine prostate tumor tissues

To investigate the *BMP9*, *ALK1* and *ALK2* expression in human prostate cancer samples we performed bioinformatics analysis using data mining platforms (R2: microarray analysis and visualization platform http://r2.amc.nl, source: GEO ID: gse29079) of mRNA expression of *ALK1*, *ALK2* receptor and *BMP9* ligand (**Fig.S3D-F**) in 48 benign tumors versus 47 malignant prostate tumors[45]. Levels of *ALK1* transcripts are decreased in the malignant tumor group compared to the benign group ($p<0.001$). Interestingly, levels of *ALK2* transcripts are significantly increased ($p<0.01$) in the malignant tumor group compared to the benign group, thus correlating with disease progression, while *BMP9* mRNA expression is similar in both groups ($p=0.28$). Previously, cDNA microarray analysis was performed in the study of Bacac *et al.,*[46] using laser-microdissected stromal cells from murine prostate intraepithelial neoplasia (PIN) and invasive prostate tumors.
Analysis of *ALK1*, *ALK2* and *BMP9* expression (**Fig.S3G-I**) in this dataset indicated elevated mRNA expression of *ALK1* and similarly increased expression of both *ALK2* and *BMP9* during the invasive stage of murine prostate cancer.

ALK1Fc inhibits ALDH1A1 expression *in vivo* and interferes with NOTCH signaling

Finally, given the reduction of primary tumor burden and the *in vitro* effects of the ALK1Fc on cell proliferation we assessed the relative expression of the *ALDH1A1* marker that is associated with cancer stem-like cells and poor patient prognosis[31,32]. Treatment with ALK1Fc affected the number of proliferative ALDH1A1 positive cells in the prostate tumor tissues both at protein (**Fig.3C**) and mRNA levels (**Fig.3D**). *In vitro* stimulation with BMP9 of the same cell line used to induce tumors in xenograft mouse model, confirmed that BMP9 and BMP9+CFc upregulates *ALDH1A1* expression, while BMP9+ALK1Fc treatment abolishes this effect (**Fig.3E**). Interestingly, ALDH1A1 is known to be regulated by NOTCH signaling[29-31]. The role of NOTCH1 in prostate cancer cell cell proliferation and migration has been extensively studied[28,47-50]. Larrivée *et al.,* have shown that ALK1 and NOTCH converge on common downstream pathways and that BMP9 treatment alone upregulates *JAG1* levels in human umbilical vein endothelial (HUVEC) non-transformed cells[51]. To verify the effect of BMP9 on NOTCH signaling activation in our cancer model, we quantified by qRT-PCR the expression of *JAG1* after BMP9 stimulation in presence of ALK1Fc or CFc. Our transcriptional analysis showed that BMP9 and BMP9+CFc induce mRNA expression of *JAG1* and that ALK1Fc is able to reduce the BMP9-mediated induction of *JAG1* (**Fig.4A**). To assess the clinical relevance of BMP9/ALK2-mediated NOTCH pathway activation in human prostate cancer we performed bioinformatics analysis using data mining platforms (R2: microarray analysis and visualization platform http://r2.amc.nl, source: GEO ID: gse29079). Levels of NOTCH ligand *JAG1* transcript show statistically significant enrichment in the malignant tumor group compared to the benign group (**Fig.4B**) and positively correlates with *ALK2* expression and disease progression (**Fig.4D)**. In addition, expression levels of *NOTCH1* receptor in human prostate tumor microarray data indicate a positive correlation with progression to malignancy (**Fig.4C**) and with *ALK2* expression (**Fig.4E**). Overexpression of JAG1 in PC-3M-Pro4Luc2 human prostate cancer cells seems to increase metabolic activity and total cell number as assessed by MTS assay (**Fig.4F**).
Knockdown of the NOTCH1 receptor in PC-3M-Pro4Luc2 (shNOTCH1), validated by western immunoblotting for NOTCH1 protein detection (**Fig.S4A**) and NOTCH reporter (RBP-JK-

luc) assay (**Fig.S4B**), showed reduced mRNA levels of *JAG1* (**Fig.S4C**) and decreased cell proliferation, as compared to cells transduced with non-targeting shRNA lentivirus ($p<0.05$ at 48 hrs) (**Fig.4G**). Stimulation of shNOTCH1-knockdown cell line with BMP9 increases their cell growth rate (**Fig.4H**) overcoming the knockdown of NOTCH1. Our data therefore suggest that BMP9/ ALK2 directly induces activation of NOTCH downstream target genes (JAG1) likely in a NOTCH1-independent way[45,52,53] which leads to higher cell proliferation and is associated with tumor progression in PCa.

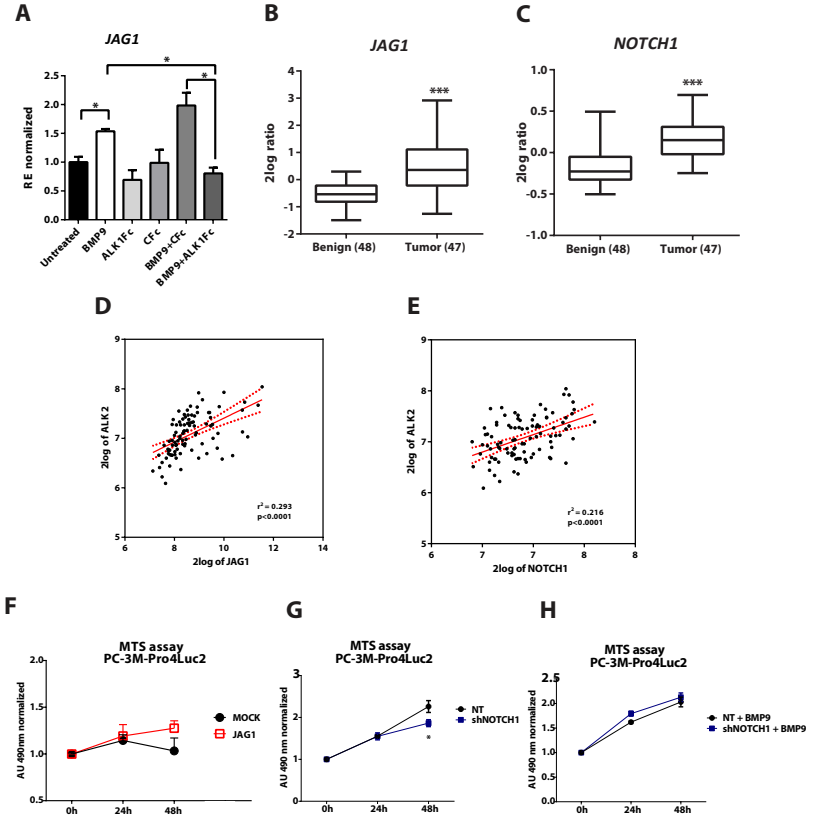

Fig.4. Effect of BMP9 and ALK1Fc on NOTCH signaling pathway and correlation study
(A). Expression of *JAG1* in PC-3M-Pro4Luc2 cells. Relative mRNA expression was measured by Q-PCR from cDNA obtained from PC-3M-Pro4Luc2 cells treated with BMP9, ALK1Fc, CFc, BMP9+ALK1Fc or BMP9+CFc for 96 hours. Values are normalized to *β-actin* expression. Error bars are ±SEM (n=3). (B-C). Bioinformatics analysis of AMC OncoGenomics database (Sueltman transcript comparison) showing mRNA expression of *JAG1* (B) and *NOTCH1* (C) and in prostate tissues among benign prostate tissues (n=48) versus tumor tissues (n=47). Values are expressed as 2log ratio tumor/ benign. ns: non-significant. P value < 0.001 (***). (D). Correlation analysis of *JAG1* and *ALK2* expression ($p<0.0001$) and (E). correlation analysis of *NOTCH1* and *ALK2* expression ($p<0.0001$) in prostate tissues among benign prostate tissues (n=48) versus tumor tissues (n=47). Bioinformatic analysis was performed using the AMC OncoGenomics database (Sueltman transcript comparison), values are expressed as 2log ratio tumor/ benign. ns: non-significant. (F). Cell numbers were assessed by MTS assay (0, 24 and 48 hours) in PC-3M-Pro4Luc2 cells transfected with 1ug JAG1 or Mock expression vector (n=2). (G-H). Cell numbers were assessed by MTS assay (0, 24 and 48 hours). PC-3M-Pro4Luc2 cells were transduced with short hairpin RNA against NOTCH1 (shNOTCH1) lentiviral vector or non-targeting (NT) shRNA vector (mock) and plated at low density. Treatment with BMP9 (1nM) was done once at cell seeding (t=0) MTS absorbance was measured. Values are normalized to the basal measurements t=0 after cell seeding and treatments. Graph represents values from four independent experiments (n=4). Error bars indicate SEM. P value <0.05 (*).

Discussion

In this study, BMP9 was found to have a tumor- promoting effect on human prostate cancer cell *in vitro* and *in vivo*. We demonstrated here that blocking of BMP9 with ALK1Fc ligand trap efficiently diminished BMP9-driven cell proliferation in human prostate cancer cells and significantly reduced tumor growth in orthotopic model of human prostate cancer.
BMP9 was first identified in the liver[15] and active forms are present in serum[13]. BMP9 is a ligand for the ALK1 receptor in endothelial cells[10] and has been shown to exert both stimulatory and inhibitory effects on endothelial cell type growth and migration[36,54]. Aberrant regulation of the TGFβ and BMP signaling pathway members often results in cancer progression[55,56]. In particular, BMP ligands, such as BMP9 as well as BMP type I receptors (e.g. ALK1 and ALK2) have been associated with tumor angiogenesis and cancer progression. In non-endothelial cells, BMP9 signals through ALK2 receptor such as in ovarian epithelium, where it has been shown to promote ovarian cancer cell proliferation[13]. Similarly, in hepatocellular carcinoma BMP9 has been reported to act as proliferative and survival factor[17]. In breast cancer few studies have highlighted the role of BMP9 in reducing breast cancer cells growth and metastasis[57-59]. However, the role of BMP9 and ALKs, in promoting or suppressing different cancer types, remains controversial. Collectively, these indicate that the effect of BMP9 on tumor promotion versus tumor suppression might be cancer-type specific, thus providing the rationale to elucidate the role of BMP9 in prostate cancer, for which little information is available to our knowledge.
Using publicly available databases of human prostate cancer specimens, we found that ALK2 is significantly upregulated in malignant versus benign tumor tissue samples, whereas ALK1 is significant downregulated, supporting the notion that the tumor-promoting effect of BMP9 is mediated by ALK2 as in our model[45]. Additionally, microarray analysis of data from mouse prostate intraepithelial neoplasia (PIN) versus invasive cancer in a multistage model of prostate carcinogenesis showed upregulation of ALK2 and BMP9 at the invasive stage in the stromal compartment[60]. Taken together, these data suggest a tumor-promoting role of BMP9 produced by the supportive stroma during prostate cancer progression. The fact that the BMP9 transcript levels registered in the selected dataset are similar in benign versus tumor stage in human prostate tumor samples, suggest a paracrine effect of BMP9 in human prostate cancer[45]. The significant increased expression of ALK2 in human prostate tumor tissue samples suggest that the BMP9 produced by the stromal compartment might be responsible for the tumor promoting effect that we documented here.
Our *in vitro* findings strengthen the afore-mentioned expression data and suggest that BMP9 exerts a proliferative effect in human prostate cancer cells. Moreover, functional blocking of ALK2 activity by LDN193189 supports the notion that ALK2 is critically involved in mediating this BMP9 effect. As depicted in the supplementary data, ALK1Fc and LDN193189 alone did not affect cell proliferation of human prostate cancer cells, thus, suggesting a paracrine effect of stroma-derived BMP9 on tumor cells. BMP9 does not influence clonogenic ability of human prostate cancer cells but a significant stimulatory effect on the colony size was observed, suggesting an influence on colony expansion rather than on colony formation.
In the orthotopic model of human prostate cancer used in this study, ALK1Fc significantly reduced the prostate tumor burden compared to control group. Strikingly, ALK1Fc treatment of tumor- bearing animals resulted in highly hypoxic tumors and a trend for decreased number of CD31+ tumor capillaries, thus supporting the notion that ALK1Fc could possibly block BMP9-induced neovascularization. Additionally, vascular density manifested by

lectin may suggest an overall reduced trend in lectin- positive area in animals treated with ALK1Fc versus CFc. Lectin distribution appeared to be less diffused, suggesting that ALK1Fc treatment contributes to vessel integrity and maintenance rather than angiogenesis.
As expected, areas of tumor cell proliferation and apoptosis were found to be mutually exclusive distribution, with apoptotic regions highly, but not completely, overlapping with the hypoxic areas, suggesting that blocking of BMP9 by ALK1Fc might have an effect on cell proliferation and apoptosis of human prostate cancer cells besides targeting vessel maintenance[34].
SMAD1 and SMAD5 (effectors of BMP9 signaling) can directly interact with JAG1 promoter, following BMP9 treatment[61]. BMP9 stimulation of SMAD signaling induces transcription of NOTCH ligand JAG1[51]. Transcriptional analysis revealed that ALK1Fc systemically blocked the induction of *JAG1* mRNA in presence of BMP9[61] at latest time point. We hypothesized that the crosstalk between BMP9 and NOTCH has translational implications in prostate cancer. *In silico* analysis of previously published dataset of human prostate cancer specimens, confirmed upregulation of *NOTCH1* and *JAG1* at the tumor stage[45]. Database analysis in a multistage model of prostate carcinogenesis on mouse prostate intraepithelial neoplasia (PIN) versus invasive cancer also indicated that *Jag1* is significantly upregulated in the stroma of invasive cancer stage[60].
Interestingly, NOTCH activates aldehyde dehydrogenase 1A1 (ALDH1A1), which is a well-known marker of highly tumorigenic prostate cancer stem-like cells[29-31]. This subpopulation contributes to both initiation and progression of the cancer and when highly expressed in advanced-stage correlates with poor survival in hormone-naïve patients[31]. ALK1Fc treated tumours showed significant reduction of ALDH1A1, which in combination with the data described above, suggest that ALK1Fc might potentially interfere with NOTCH signaling in the regulation of ALDH1A1. In conclusion, our findings provide novel information on the role of BMP9 in human prostate cancer and suggest the promising use of BMP9 targeting molecules for the treatment of tumor and supportive microenvironment in prostate cancer patients.

Supplementary Material

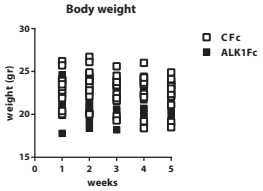

Fig.S1. Body weight of animals used in the *in vivo* experiment
Body weight (grams) of all the animals of treatment groups measured weekly during the course of treatment with either CFc (n=6) (A) or ALK1Fc (n=7).

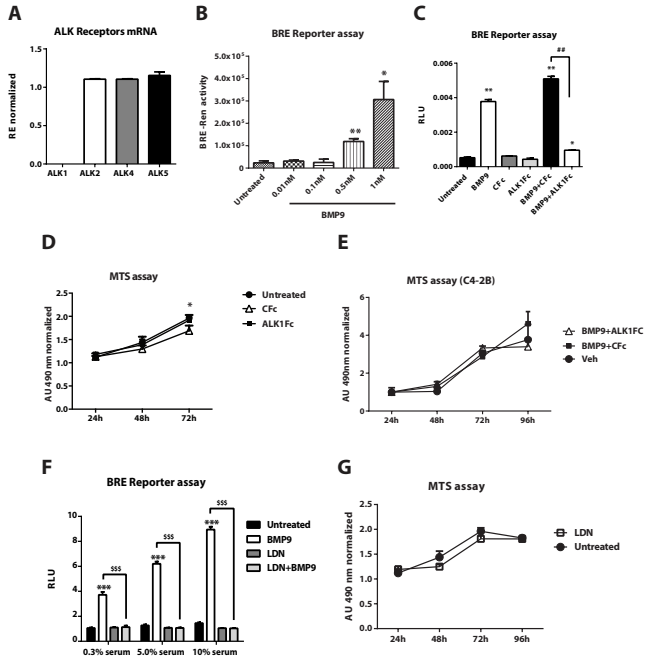

Fig. S2. Characterization of BMP9 response *in vitro*
(A). Endogenous expression of *ALK1*, *ALK2*, *ALK4* and *ALK5* receptors in PC-3M-Pro4Luc2cells (mRNA level). Relative expression levels normalized to β-actin are shown. Error bars indicate +/-SD. (B). Dose dependent response of PC-3M-Pro4Luc2 cells to recombinant BMP9 (0.01, 0.1, 0.5, 1 nM). Downstream activation of BMP signaling was tested by transfection of BRE-renilla construct and measured by reporter activity assay. Graph represents values from three independent experiments; error bars indicate ± SEM (n=3). P value < 0.05 (*) and P value < 0.01 (**). (C). BRE reporter luciferase (BRELuc) assay; Inhibitory concentration of ALK1Fc or CFc (10ug/ml) was determined in cells stimulated with 1nM BMP9. Graph represents values from two independent experiments; error bars indicate ± SEM (n=2). P value < 0.05 (*) and P value < 0.01 (**) compared to "untreated" control. P value < 0.01 (##) (D). MTS assay (24, 48, 72 hours) was performed in PC-3M-Pro4-luc2 human prostate cancer cell line treated with recombinant ALK1Fc (10ug/ml), CFc (10ug/ml). Accumulation of MTS was measured based on absorbance at 490 nm. Values are normalized to the basal measurements at 24 hours after cell seeding and treatments. Graph represents values from two independent experiments (n=2). Error bars indicate ±SEM. (E). MTS assay (24, 48, 72, 96 hours) was performed in C4-2B human prostate cancer cell lines stimulated with recombinant BMP9 (1nM), BMP9 (1nM)+ALK1Fc (10ug/ml) or BMP9 (1nM)+CFc (10ug/ml). (n=3). (F). BMP transcriptional reporter assay (BRE-luciferase). PC-3M-Pro4 were seeded and, transfected with BRE-luc and renilla plasmid DNA. After 24 hours the medium was replaced with 0.3%, 5%, 10% FCII serum containing media and treated with BMP9 (1nM), LDN193189 (LDN, 120nM) and BMP9+LDN. Luc and Ren values were measured 24 hrs after treatment. RLU ratio values are shown (Luc/Ren). Error bars indicate ±SD. (G). MTS assay (24, 48, 72 hours) was performed in PC-3M-Pro4-luc2 human prostate cancer cell line treated with LDN inhibitor (LDN193189, 120nM). (n=2). Error bars indicate +/-SEM.

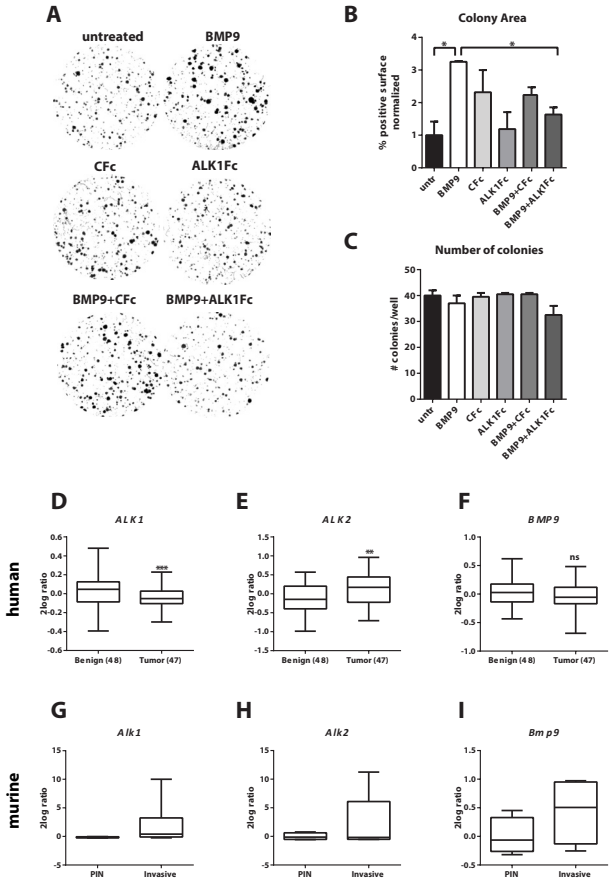

Fig. S3. Effect of BMP9 and ALK1Fc on clonogenicity and ALK expression in human samples
(A). Clonogenic assay of PC-3M-Pro4Luc2 cells. Low-density cultures (100 cells per well of 6well plate) were stimulated with BMP9, CFc, ALK1Fc, BMP9+CFc, BMP9+ALK1Fc. Colony formation was assessed after 10 days by crystal violet staining. Representative images are shown. (B-C). Quantification of surface covered by crystal violet positive colonies (colony area) and colony number. Graph shows percentage of positive surface normalized per condition (average of three independent experiments). P value < 0.05 (*), ns; non-significant. Error bars indicate SEM. (D-F). Bioinformatics analysis of AMC OncoGenomics database (Sueltman transcript comparison) showing mRNA expression of *ALK1*, *ALK2* and *BMP9* in prostate tissues among benign prostate tissues (n=48) versus tumor tissues (n=47). Values are expressed as 2log ratio tumor/ benign. ns: non-significant. P value < 0.01 (**) (G-I). Microarray cDNA analysis (adapted from Bacac *et al.,* **[46]**) of *Alk1*, *Alk2* and *Bmp9* expression in microdissected murine stroma derived from two tumor stages; prostate intraepithelial neoplasia (PIN, n=4), and invasive tumors (n=6).

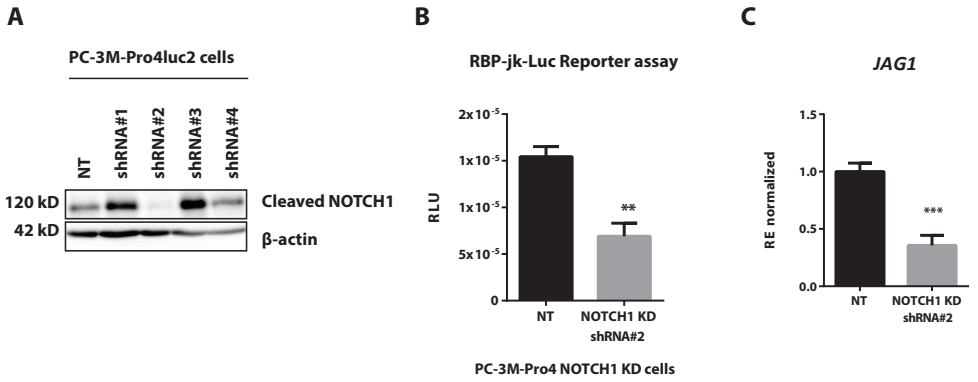

Fig.S4.Characterization of NOTCH1 knock-down
(A). Western immunoblotting for NOTCH1 protein as validation of lentiviral shRNA-mediated knockdown of NOTCH1 intracellular domain (cleaved) in PC-3M-Pro4luc2 PCa cell line using five shRNA constrcuts. Based on the downregulation of cleaved NOTCH1 observed after lentiviral transduction and puromycin selection, the stable line expressing the shRNA #2 construct was selected for further experiments. NT; non-targeting shRNA lentiviral mediated transduction. β-actin was used as loading control. (B). NOTCH transcription factor RBP-Jk-luciferase reporter assay in non-targeting (NT) and NOTCH1 (shRNA#2) knockdown (KD) PC-3M-Pro4Luc2 cells. RLU: relative luciferase units (signal of luciferase normalised to renilla values). n=3, P value < 0.01 (**)
(C). QPCR for *JAG1* mRNA levels in non-targeting (NT) and NOTCH1 (shRNA#2) knockdown (KD) PC-3M-Pro4Luc2 cells. Fold over the value of NT is represented. Error bars indicate ±SD. P value < 0.001 (***).

Acknowledgements
The research leading to these results has received funding from the FP7 Marie Curie ITN under grant agreement No. 264817- BONE-NET (EZ) and from the Netherlands Initiative of Regenerative Medicine (NIRM, grant No. FES0908). We would also like to thank Marjan van de Merbel.

References

1. Jemal, A., et al., Global patterns of cancer incidence and mortality rates and trends. Cancer Epidemiol Biomarkers Prevent, 2010. 19(8): p. 1893-907.
2. Chang, A.J., et al., High-risk prostate cancerclassification and therapy. Nat Rev Clin Oncol, 2014. 11(6): p. 308-323.
3. http://www.cancer.gov/types/prostate/hp/prostate-treatment-pdq#section/_1.
4. Barlow, L.J. and M.M. Shen, Snapshot: prostate cancer. Cancer Cell, 2013. 24(3): p. 400-401.
5. Chen, Y., N.J. Clegg, and H.I. Scher, Anti-androgens and androgen-depleting therapies in prostate cancer: new agents for an established target. Lancet Oncol, 2009. 10(10): p. 981-991.
6. Nelson, W.G., A.M. De Marzo, and W.B. Isaacs, Prostate cancer. N Engl J Med, 2003. 349(4): p. 366-381.
7. Redig, A.J. and S.S. McAllister, Breast cancer as a systemic disease: a view of metastasis. J Intern Med, 2013. 274(2): p. 113-126.
8. Bendell, J.C., et al., Safety, pharmacokinetics, pharmacodynamics, and antitumor activity of dalantercept, an activin receptor-like kinase-1 ligand trap, in patients with advanced cancer. Clin Cancer Res, 2014. 20(2): p. 480-9.
9. Hawinkels, L.J., A. Garcia de Vinuesa, and P. Ten Dijke, Activin receptor-like kinase 1 as a target for anti-angiogenesis therapy. Expert Opin Investig Drugs, 2013. 22(11): p. 1371-83.
10. van Meeteren, L.A., et al., Anti-human Activin receptor-like kinase 1 (ALK1) antibody attenuates Bone morphogenetic protein 9 (BMP9)-induced ALK1 signaling and interferes with endothelial cell sprouting. J Biol Chem, 2012. 287(22): p. 18551-18561.
11. Bragdon, B., et al., Bone morphogenetic proteins: a critical review. Cell Signal, 2011. 23(4): p. 609-620.
12. David, L., et al., Identification of BMP9 and BMP10 as functional activators of the orphan activin receptor-like kinase 1 (ALK1) in endothelial cells. Blood, 2007. 109(5): p. 1953-61.
13. Herrera, B., et al., Autocrine bone morphogenetic protein-9 signals through activin receptor-like kinase-2/Smad1/Smad4 to promote ovarian cancer cell proliferation. Cancer Res, 2009. 69(24): p. 9254-62.
14. Scharpfenecker, M., et al., BMP-9 signals via ALK1 and inhibits bFGF-induced endothelial cell proliferation and VEGF-stimulated angiogenesis. J Cell Sci, 2007. 120(Pt 6): p. 964-72.
15. Celeste AJ, S.J., Cox K, Rosen V, Wozney JM, Bone morphogenetic protein-9, a new member of the TGF-β superfamily. J Bone Min Res, 1994. 1(136).
16. Song, J.J., et al., Bone morphogenetic protein-9 binds to liver cells and stimulates proliferation. Endocrinology, 1995. 136(10): p. 4293-4297.
17. Herrera, B., et al., BMP9 is a proliferative and survival factor for human hepatocellular carcinoma cells. PLoS One, 2013. 8(7): p. e69535.
18. Li, R., et al., Targeting BMP9-promoted human osteosarcoma growth by inactivation of notch signaling. Curr Cancer Drug Targets, 2014. 14(3): p. 274-85.
19. Wang, K., et al., BMP9 inhibits the proliferation and invasiveness of breast cancer cells MDA-MB-231. J Cancer Res Clin Oncol, 2011. 137(11): p. 1687-1696.
20. Ye, L., H. Kynaston, and W.G. Jiang, Bone morphogenetic protein-9 induces apoptosis in prostate cancer cells, the role of prostate apoptosis response-4. Mol Cancer Res, 2008. 6(10): p. 1594-1606.
21. Olsen, O.E., et al., Bone morphogenetic protein-9 suppresses growth of myeloma cells by signaling through ALK2 but is inhibited by endoglin. Blood Cancer J, 2014. 4: p. e196.
22. Cunha, S.I. and K. Pietras, ALK1 as an emerging target for antiangiogenic therapy of cancer. Blood, 2011. 117(26): p. 6999-7006.
23. Urness, L.D., L.K. Sorensen, and D.Y. Li, Arteriovenous malformations in mice lacking activin receptor-like kinase-1. Nat Genet, 2000. 26(3): p. 328-31.
24. Gale, N.W., et al., Haploinsufficiency of delta-like 4 ligand results in embryonic lethality due to major defects in arterial and vascular development. Proc Natl Acad Sci U S A, 2004. 101(45): p. 15949-54.
25. Krebs, L.T., et al., Haploinsufficient lethality and formation of arteriovenous malformations in Notch pathway mutants. Genes Dev, 2004. 18(20): p. 2469-73.
26. Carvalho, F.L., et al., Notch signaling in prostate cancer: a moving target. Prostate, 2014. 74(9): p. 933-45.
27. Ross, A.E., et al., Gene expression pathways of high grade localized prostate cancer. Prostate, 2011.
28. Wang, Z., et al., Down-regulation of Notch-1 and Jagged-1 inhibits prostate cancer cell growth, migration and invasion, and induces apoptosis via inactivation of Akt, mTOR, and NF-kappaB

signaling pathways. J Cell Biochem, 2010. 109(4): p. 726-36.
29. Zhao, D., et al., NOTCH-induced aldehyde dehydrogenase 1A1 deacetylation promotes breast cancer stem cells. J Clin Invest, 2014. 124(12): p. 5453-65.
30. Ginestier, C., et al., ALDH1 is a marker of normal and malignant human mammary stem cells and a predictor of poor clinical outcome. Cell Stem Cell, 2007. 1(5): p. 555-67.
31. Le Magnen, C., et al., Characterization and clinical relevance of ALDH bright populations in prostate cancer. Clin Cancer Res, 2013. 19(19): p. 5361-71.
32. Li, T., et al., ALDH1A1 is a marker for malignant prostate stem cells and predictor of prostate cancer patients' outcome. Lab Invest, 2010. 90(2): p. 234-44.
33. Seehra, J., et al., Antagonists of Bmp9, Bmp10, Alk1 and other Alk1 ligands, and uses thereof (International Patent WO2009139891). 2009.
34. Mitchell, D., et al., ALK1-Fc inhibits multiple mediators of angiogenesis and suppresses tumor growth. Mol Cancer Ther, 2010. 9(2): p. 379-88.
35. Cunha, S.I., et al., Genetic and pharmacological targeting of activin receptor-like kinase 1 impairs tumor growth and angiogenesis. J Exp Med, 2010. 207(1): p. 85-100.
36. Suzuki, Y., et al., BMP-9 induces proliferation of multiple types of endothelial cells in vitro and in vivo. J Cell Sci, 2010. 123(10): p. 1684-1692.
37. Kroon, J., et al., Glycogen synthase kinase-3β inhibition depletes the population of prostate cancer stem/progenitor-like cells and attenuates metastatic growth. Oncotarget, 2014. 5(19): p. 8986-94.
38. Korchynskyi, O. and P. ten Dijke, Identification and functional characterization of distinct critically important Bone morphogenetic protein-specific response elements in the Id1 promoter. J Biol Chem, 2002. 277(7): p. 4883-4891.
39. Berridge, M.V., P.M. Herst, and A.S. Tan, Tetrazolium dyes as tools in cell biology: new insights into their cellular reduction, in Biotechnology Annual Review. 2005, Elsevier. p. 127-152.
40. van der Pluijm, G., et al., Interference with the microenvironmental support impairs the de novo formation of bone metastases in vivo. Cancer Res, 2005. 65(17): p. 7682-90.
41. Karkampouna, S., et al., Novel ex vivo culture method for the study of Dupuytren's Disease: effects of TGFβ type 1 receptor modulation by antisense oligonucleotides. Mol Ther Nucleic Acids, 2014. 3: p. e142.
42. Craft, C.S., et al., Endoglin inhibits prostate cancer motility via activation of the ALK2-Smad1 pathway. Oncogene, 2007. 26(51): p. 7240-50.
43. Shi, S., et al., BMP antagonists enhance myogenic differentiation and ameliorate the dystrophic phenotype in a DMD mouse model. Neurobiol Dis, 2011. 41(2): p. 353-60.
44. Cuny, G.D., et al., Structure-activity relationship study of bone morphogenetic protein (BMP) signaling inhibitors. Bioorg Med Chem Lett, 2008. 18(15): p. 4388-92.
45. Borno, S.T., et al., Genome-wide DNA methylation events in TMPRSS2-ERG fusion-negative prostate cancers implicate an EZH2-dependent mechanism with miR-26a hypermethylation. Cancer Discov, 2012. 2(11): p. 1024-35.
46. Bacac, M., et al., A mouse stromal response to tumor invasion predicts prostate and breast cancer patient survival. PLoS One, 2006. 1(1): p. e32.
47. Shou, J., et al., Dynamics of notch expression during murine prostate development and tumorigenesis. Cancer Res, 2001. 61(19): p. 7291-7.
48. Zhang, Y., et al., Down-regulation of Jagged-1 induces cell growth inhibition and S phase arrest in prostate cancer cells. Int J Cancer, 2006. 119(9): p. 2071-7.
49. Leong, K.G. and W.Q. Gao, The Notch pathway in prostate development and cancer. Differentiation, 2008. 76(6): p. 699-716.
50. Bin Hafeez, B., et al., Targeted knockdown of Notch1 inhibits invasion of human prostate cancer cells concomitant with inhibition of matrix metalloproteinase-9 and urokinase plasminogen activator. Clin Cancer Res, 2009. 15(2): p. 452-9.
51. Larrivee, B., et al., ALK1 signaling inhibits angiogenesis by cooperating with the Notch pathway. Dev Cell, 2012. 22(3): p. 489-500.
52. Ricard, N., et al., BMP9 and BMP10 are critical for postnatal retinal vascular remodeling. 2012. 119(25): p. 6162-6171.
53. Kerr, G., et al., A small molecule targeting ALK1 prevents Notch cooperativity and inhibits functional angiogenesis. Angiogenesis, 2015.
54. David, L., et al., Identification of BMP9 and BMP10 as functional activators of the orphan activin

receptor-like kinase 1 (ALK1) in endothelial cells. Blood 2007. 109(5): p. 1953-1961.
55. Siegel, P.M. and J. Massague, Cytostatic and apoptotic actions of TGFβ in homeostasis and cancer. Nat Rev Cancer, 2003. 3(11): p. 807-820.
56. Massagué, J., TGFβ in Cancer. Cell, 2008. 134(2): p. 215-230.
57. Wang, K., et al., BMP9 inhibits the proliferation and invasiveness of breast cancer cells MDA-MB-231. J Cancer Res Clin Oncol, 2011. 137(11): p. 1687-96.
58. Ren, W., et al., BMP9 inhibits the bone metastasis of breast cancer cells by downregulating CCN2 (connective tissue growth factor, CTGF) expression. Mol Biol Rep, 2014. 41(3): p. 1373-83.
59. Ren, W., et al., BMP9 inhibits proliferation and metastasis of HER2-positive SK-BR-3 breast cancer cells through ERK1/2 and PI3K/AKT pathways. PLoS One, 2014. 9(5): p. e96816.
60. Bacac, M., et al., A mouse stromal response to tumor invasion predicts prostate and breast cancer patient survival. PLoS One, 2006. 1: p. e32.
61. Morikawa, M., et al., ChIP-seq reveals cell type-specific binding patterns of BMP-specific Smads and a novel binding motif. Nucleic Acids Res, 2011. 39(20): p. 8712-27.